Developmental Cell
Article

Transcriptional Mechanisms Link Epithelial Plasticity to Adhesion and Differentiation of Epidermal Progenitor Cells

Briana Lee,[1] Alvaro Villarreal-Ponce,[1] Magid Fallahi,[1] Jeremy Ovadia,[2] Peng Sun,[1] Qian-Chun Yu,[3] Seiji Ito,[4] Satrajit Sinha,[5] Qing Nie,[2] and Xing Dai[1,*]
[1]Department of Biological Chemistry, School of Medicine
[2]Department of Mathematics
University of California, Irvine, Irvine CA 92697, USA
[3]Department of Pathology and Laboratory Medicine, University of Pennsylvania, Philadelphia, PA 19104, USA
[4]Department of Medical Chemistry, Kansai Medical University, Moriguchi 570-8506, Japan
[5]Department of Biochemistry, State University of New York, Buffalo, NY 14260, USA
*Correspondence: xdai@uci.edu
http://dx.doi.org/10.1016/j.devcel.2014.03.005

SUMMARY

During epithelial tissue morphogenesis, developmental progenitor cells undergo dynamic adhesive and cytoskeletal remodeling to trigger proliferation and migration. Transcriptional mechanisms that restrict such a mild form of epithelial plasticity to maintain lineage-restricted differentiation in committed epithelial tissues are poorly understood. Here, we report that simultaneous ablation of transcriptional repressor-encoding *Ovol1* and *Ovol2* results in expansion and blocked terminal differentiation of embryonic epidermal progenitor cells. Conversely, mice overexpressing Ovol2 in their skin epithelia exhibit precocious differentiation accompanied by smaller progenitor cell compartments. We show that *Ovol1/Ovol2*-deficient epidermal cells fail to undertake α-catenin-driven actin cytoskeletal reorganization and adhesive maturation and exhibit changes that resemble epithelial-to-mesenchymal transition (EMT). Remarkably, these alterations and defective terminal differentiation are reversed upon depletion of EMT-promoting transcriptional factor Zeb1. Collectively, our findings reveal Ovol-Zeb1-α-catenin sequential repression and highlight Ovol1 and Ovol2 as gatekeepers of epithelial adhesion and differentiation by inhibiting progenitor-like traits and epithelial plasticity.

INTRODUCTION

A fundamental question in developmental biology is how epithelial cells maintain dynamic yet stable intercellular adhesions to support tissue morphogenesis (Maiden and Hardin, 2011). Mammalian skin epithelia offer a prime model system to address this. The epidermis and its associated appendages (e.g., hair follicle or HF) develop from a single-layered surface ectoderm during embryogenesis (Koster et al., 2007). Following commitment, epidermal basal cells either differentiate, delaminate, and migrate up to become suprabasal cells, or divide asymmetrically to produce a proliferative daughter cell that remains basal and a transiently proliferative spinous cell that assumes a suprabasal location (Fuchs, 2008). In upward movement, spinous cells differentiate into granular keratinocytes, which go on to produce the outermost stratum corneum constituting a vital permeability barrier. Likewise, committed HF cells undergo expansion and first downward then upward migration on their journey to produce a hair shaft (Jamora and Fuchs, 2002). Epidermal and HF stem/progenitor cells face the challenging need of dampening intercellular adhesions to promote proliferation and migration while achieving stable cell-cell contacts upon tissue maturation (Fuchs, 2007). Adherens junctions and their associated proteins such as E-cadherin (Ecad) and α-catenin lie at the heart of these dynamics (Fuchs and Nowak, 2008). Consistently, ablation of *Cdh1* (Ecad) or *Ctnna1* (α-catenin) in the epidermis results in abnormal intercellular adhesion, hyperproliferation, and altered differentiation (Tinkle et al., 2004; Vasioukhin et al., 2000, 2001). The resulting defects are significantly more dramatic for the loss of α-catenin, in keeping with its central role in integrating cell adhesion and actin cytoskeleton dynamics with growth signaling (Maiden and Hardin, 2011). To date, transcriptional mechanisms regulating adherens junction proteins have been largely focused on Ecad, whereas the regulation of α-catenin has been thought to occur through genetic mutations and/or posttranslational mechanisms (Kobielak and Fuchs, 2004).

Interesting parallels exist between the afore-described developmental epithelial plasticity in skin and the process of epithelial-to-mesenchymal transition (EMT) (Jamora and Fuchs, 2002; Kalluri and Weinberg, 2009). During EMT, epithelial cells lose cell-cell junctions and apical-basal polarity, reorganize their cytoskeleton and shape, gain increased motility, and become mesenchymal cell types. Central to promoting the EMT program are transcription factors of the Snail, Twist, and Zeb families (Thiery et al., 2009; Yang and Weinberg, 2008). Developing skin epithelia express EMT-promoting factors: Snail is transiently expressed in HF primordia, and Slug is expressed in embryonic

epidermal basal cells (Jamora et al., 2005; Shirley et al., 2010). *K14* promoter-directed overexpression of Snail results in epidermal hyperproliferation and downregulation of Ecad (Jamora et al., 2005), whereas *Slug* null mice show delayed HF development and a thinner epidermis (Shirley et al., 2010). Whether these EMT factors act by promoting physiological adhesive and cytoskeletal remodeling during morphogenesis remains to be demonstrated. More importantly, the molecular mechanisms that restrict developmental epithelial plasticity to ensure coordinated proliferation and differentiation of skin epithelial progenitor cells are complete unknowns.

The Ovo family of zinc finger transcription factors constitutes a downstream hub of signaling pathways, including Wg/Wnt, epidermal growth factor (EGF), and bone morphogenetic protein (BMP)/transforming growth factor β (TGF-β) (Descargues et al., 2008; Gomis et al., 2006; Li et al., 2002b; Nair et al., 2006; Payre et al., 1999; Zhang et al., 2013). *Ovol1* null mice display epithelial anomalies including mildly hyperproliferative epidermis, abnormal hair shafts, defective spermatogenesis, and kidney cysts (Dai et al., 1998; Li et al., 2005; Nair et al., 2006; Teng et al., 2007), whereas *Ovol2* null mice die during midgestation (Mackay et al., 2006). In this work, we report studies that uncover compensatory/redundant roles of *Ovol1* and *Ovol2* as negative regulators of a progenitor cell state and positive regulators of terminal differentiation in at least two skin epithelial lineages: interfollicular epidermis and HFs. Moreover, we provide compelling evidence that Ovol1/Ovol2 promote the differentiation of epidermal progenitor cells in part by inhibiting EMT pathway components such as Zeb1, which in turn represses *Ctnna1* (α-catenin) transcription. These findings open the door to understanding the molecular control of developmental epithelial plasticity and epidermal differentiation by studying the involvement of other classical EMT regulators.

RESULTS

Simultaneous Ablation of *Ovol1* and *Ovol2* Results in Defective Maturation of Embryonic Epidermis and HFs

In addition to *Ovol1* (Li et al., 2002a; Nair et al., 2006), *Ovol2* is also expressed in epidermal and HF progenitor cells as they mature during embryogenesis. Nuclear Ovol2 is present predominantly in basal but also a few suprabasal epidermal cells, as well as in the down-growing front of developing HFs (Figure 1A). When epidermal cells were laser captured for RNA analysis, a significant increase in *Ovol2* mRNA was seen from embryonic day 13.5 (E13.5) to E16.5 (Figure 1B). To investigate *Ovol2* function in skin, we generated skin epithelia-specific *Ovol2* knockout (SSKO: $Ovol2^{f/-}$/*K14-Cre*) mice (Figure S1A available online). These mice developed normally, with their skin exhibiting no remarkable morphological or biochemical defects (Figures S1B and S1C) but showing a dramatically elevated level of *Ovol1* mRNA, especially in basal keratinocytes (Figures S1D and S1E). These findings, together with our previous observation of elevated *Ovol2* expression in *Ovol1*-deficient epidermis (Teng et al., 2007), raise the possibility of compensation/redundancy between *Ovol1* and *Ovol2*.

To address this, we generated *Ovol1*/*Ovol2* double-knockout (DKO: $Ovol1^{-/-}$/$Ovol2^{f/-}$/*K14*-Cre) mice. Like $Ovol1^{-/-}$ (Nair et al., 2006), DKO embryonic epidermis contained an expanded K1-positive spinous compartment (Figures 1C and 1D). Moreover, DKO epidermis displayed a number of features not observed in $Ovol1^{-/-}$. First, K5/K14/K15-positive cells expanded beyond the basal compartment, especially at earlier stages of development (Figures 1E and 1F; data not shown). Second, cells throughout the basal and spinous layers displayed abnormal morphology and shape and were often separated by notable intercellular spaces (Figures 1C and S1F). Third, the granules and cornified layers appeared immature, defects most prominently evident in electron microscopic (EM) and semithin images (Figures 1G and S1F). Consistently, the levels of late differentiation markers involucrin and filaggrin were decreased (Figure S1G). Finally, DKO epidermis failed to shed the K15-positive periderm when stratification should be complete (Figures 1C and 1F). In keeping with these maturation defects, DKO embryos lacked a functional permeability barrier, as illustrated by persistent dye penetration (Byrne et al., 1994) beyond E17.5 (Figure 1H).

HFs in DKO embryos also failed to mature properly. Compared to counterparts in control and $Ovol1^{-/-}$ skin, DKO HFs were smaller (Figure 1I), and their length was decreased (Figure 1J). Moreover, the number of HFs that express AE13, a hair keratin marker of the differentiating precortex/cortex cells, was decreased (Figure 1K). Collectively, our data reveal compensatory/redundant roles of *Ovol1* and *Ovol2* in restricting the size of the basal/spinous compartments and in facilitating terminal differentiation within both interfollicular epidermal and HF lineages.

Loss of *Ovol1*/*Ovol2* Leads to Increased Basal Cell Proliferation and Expanded Progenitor Cell Marker Expression

Next, we asked whether the expanded basal compartment in DKO epidermis associates with increased proliferation, by quantifying the number of phospho-histone H3 (pH3)-positive mitotic cells. Compared to control and $Ovol1^{-/-}$, DKO epidermis contained a higher number of mitotic cells in the basal layer (Figure 2A). To assess whether *Ovol1*/*Ovol2* play a keratinocyte-autonomous role in basal cell proliferation, we cultured primary keratinocytes from E18.5 DKO and control embryos in low-Ca^{2+} medium, which mimics the basal state. DKO keratinocytes grew more rapidly and reached confluence faster than control and $Ovol1^{-/-}$ cells (data not shown). When plated at a clonal density, DKO and $Ovol1^{-/-}$ keratinocytes produced a significantly higher number of colonies than control (Figure 2B). Thus, reducing Ovol dosage in basal cells leads them to display enhanced proliferation potential. Interestingly, whereas control and $Ovol1^{-/-}$ colonies were darkly stained with dye, reflecting a tightly packed morphology, DKO colonies were large, loose clusters of cells that were weakly stained (Figure 2B). We will return to this issue later.

To probe the underlying molecular defects, we compared gene expression between control and DKO primary keratinocytes. Consistent with known Ovol1/OVOL2 regulation of *Myc*/*MYC* (Nair et al., 2006; Wells et al., 2009), gene set enrichment analysis (GSEA) (Mootha et al., 2003) of microarray data revealed an enrichment of a MYC-activated gene set (Zeller et al., 2003) in DKO cells compared to control cells (Figure S2A). Interestingly, DKO cells also displayed an enrichment of three "stemness" gene sets (Figure S2B). MYC target and "stemness" gene sets were still enriched when proliferation/cell-cycle genes were removed from the analysis (Figures S2C and S2D), indicating

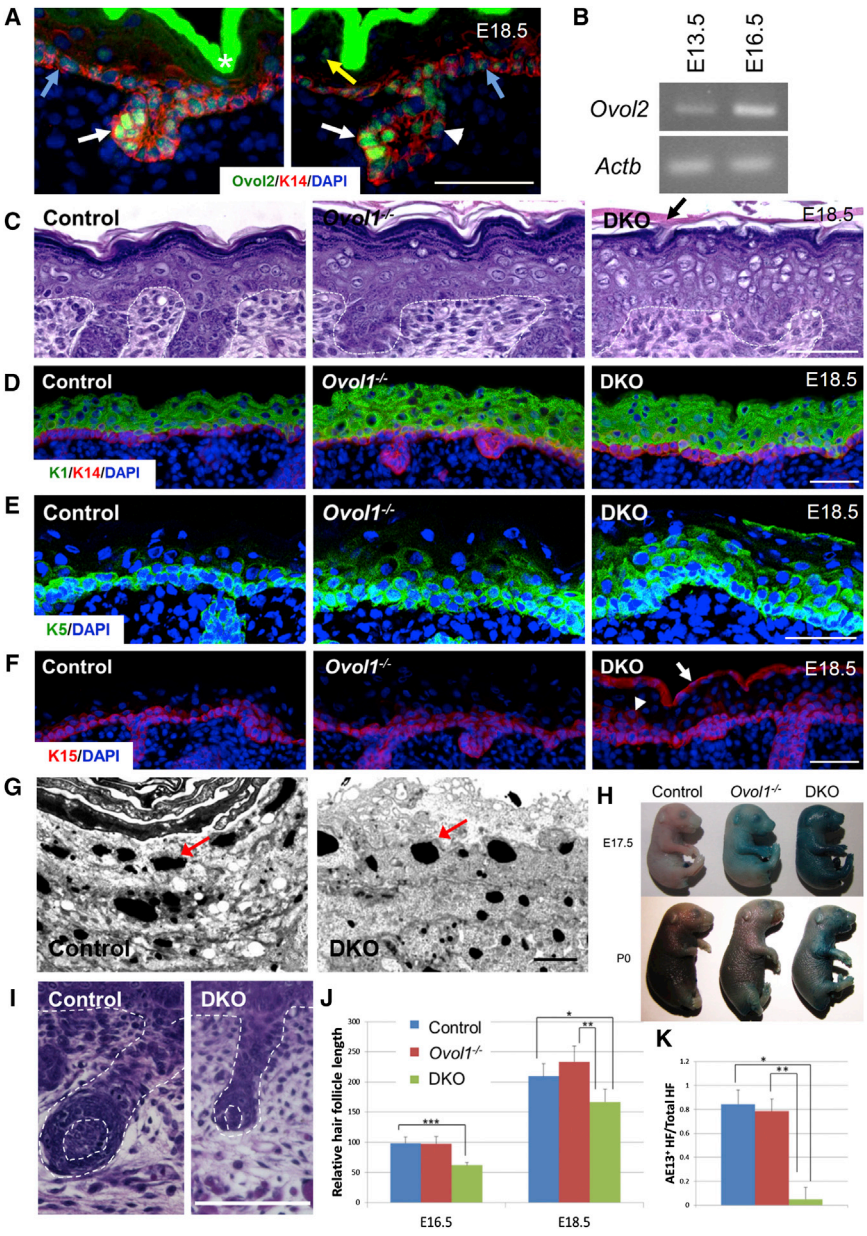

Figure 1. Loss of *Ovol1* and *Ovol2* Results in Defective Epidermal and HF Maturation

(A) Indirect immunofluorescence of Ovol2. Gray and yellow arrows point to basal and suprabasal cells, respectively. White arrows point to anterior HF cells, arrowhead points to presumptive ORS cells, and white asterisk (*) indicates nonspecific signals.

(B) Semiquantitative RT-PCR analysis of *Ovol2* mRNA at the indicated stages of development. *Actb* serves as a loading control.

(C) Hematoxylin and eosin staining (H&E).

(D–F) Indirect immunofluorescence of the indicated markers. Arrows in (C) and (F) point to the periderm. Arrowhead in (F) indicates suprabasal cells that are K15 positive. DAPI stains the nuclei.

(G) EM images of granular and cornified layers. Note that keratohyalin granules (red arrows) in DKO display a rounder, less-mature morphology.

(H) Results of dye penetration assays.

(I) Morphology of HFs at E18.5.

(J) HF length ($n \geq 2$ and $n \geq 4$ per genotype for E16.5 and E18.5, respectively). *$p = 0.01$; **$p < 0.02$; ***$p < 0.004$.

(K) Percentage of HFs that are AE13 positive in E18.5 skin ($n \geq 4$ per genotype). Genotypes are as indicated in (J). *$p < 0.0001$; **$p < 0.02$.

Error bars represent SE. Scale bars represent 25 μm (A), 50 μm (C–F and I), and 2 μm (G).

See also Figure S1.

that the enrichment was not solely due to increased proliferation. Among the enriched "stemness" genes was *Trp63* (p63), which encodes a self-renewal factor previously shown to be a master regulator of epidermal morphogenesis (Mills et al., 1999; Yang et al., 1999). RT-PCR confirmed elevated expression of *ΔNp63* (Figure S2E). Moreover, whereas nuclear p63 is normally restricted to the basal layer, it was detected not only strongly in basal but also in many suprabasal cells in DKO epidermis (Figure 2C). Sequence analysis revealed five putative Ovol binding sites in *ΔNp63* promoter (Figure 2D). In chromatin immunoprecipitation (ChIP) assays, Ovol2 bound to both *ΔNp63* and *Myc* promoters in primary keratinocytes at the predicted sites (Figure 2D). Thus, in addition to *Myc*, *ΔNp63* is likely a direct target of Ovol2.

GSEA also revealed enrichment in DKO cells of gene sets previously shown to be enriched in adult HF bulge stem cells (HF-SCs) (Lien et al., 2011) (Figure S2F). Remarkably, approximately one-quarter (24%) of the HF-SC signature was affected by *Ovol1*/*Ovol2* loss (Figure S2G). An enrichment of a basal cell carcinoma gene set was also observed (Figure S2H). Among the enriched HF-SC genes were those encoding K15 and Tcf3, which normally are also expressed in embryonic epidermal basal cells (Nguyen et al., 2006; Romano et al., 2010). We observed ectopic K15-positive cells, especially at early embryonic stages, and a persistent presence of Tcf3 in suprabasal cells in DKO epidermis (Figures 1F and 2E; data not shown). In contrast, the expression of several HF-specific/enriched SC markers, including Lrig1, Sox9, Nfatc1, and CD34 (Woo and Oro, 2011), did not exhibit any difference between control and DKO skin (Figure S3; data not shown). Collectively, these data suggest that loss of *Ovol1*/*Ovol2* results in an enhancement of molecular features associated with a primitive epidermal progenitor cell state that overlaps but is distinct from a HF-SC state.

Epithelially Directed *Ovol2* Overexpression Results in Compromised Progenitor Cell Compartments and Premature Differentiation in Developing Skin and Adult HFs

To substantiate *Ovol* function in epidermal progenitor cells, we generated *TRE-Ovol2/K5-tTA* bitransgenic (BT) mice. In the absence of doxycycline (Dox), these mice overexpress Ovol2

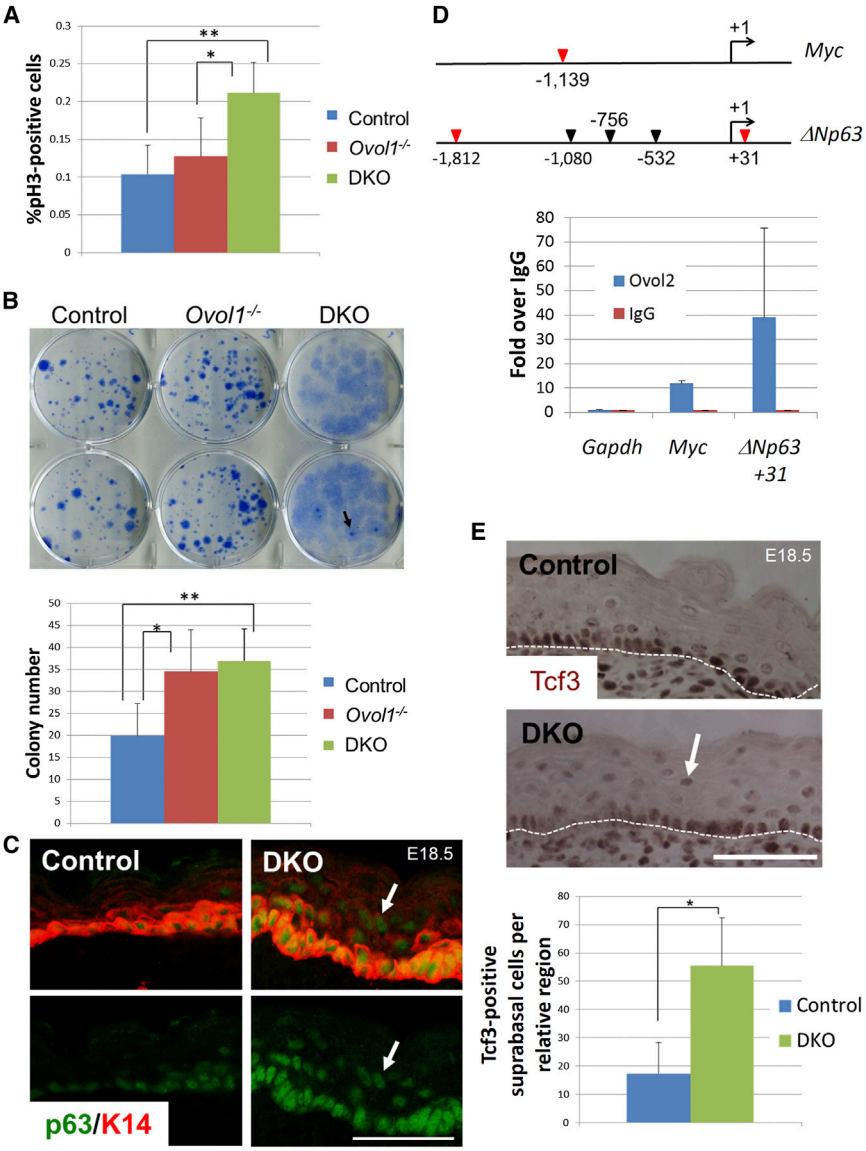

Figure 2. Increased Proliferation and Clonogenicity with Loss of *Ovol1* and *Ovol2*

(A) Basal cell proliferation. Shown are results of quantification of pH3$^+$cells in skin of the indicated genotypes (n ≥ 5 per genotype). *p < 0.08; **p < 0.0002.

(B) Morphology (top) and number (bottom) of colonies produced by keratinocytes from embryonic skin (n ≥ 4 per genotype). Arrow points to a DKO colony with dense morphology at the center reminiscent of that in a typical epithelial colony, surrounded by loose, lightly stained peripheral cells. *p < 0.01; **p < 0.0002.

(C) Immunofluorescent detection of p63. Top panels are merged images showing p63 and K14 double staining. Bottom panels show p63 staining only. Arrows point to p63-positive suprabasal cells in DKO epidermis.

(D) ChIP analysis of Ovol2 on *Myc* and *ΔNp63* (diagrams shown at the top). Triangles indicate putative Ovol sites, with validated binding sites shown in red. *Gapdh* serves as a negative control.

(E) Immunohistochemical detection of Tcf3. Dashed line indicates the basement membrane. Arrow indicates aberrant suprabasal Tcf3$^+$ cells (with their number quantified as shown at the bottom; n = 4 per genotype). *p = 0.03.

Error bars represent SE. Scale bars represent 50 μm (C and E).

See also Figures S2 and S3.

in embryonic K5-positive cells, which include the epidermal basal layer and the presumptive outer root sheath (ORS) of HFs (Byrne et al., 1994; Diamond et al., 2000) (Figure S4A). Because Ovol1 and Ovol2 recognize nearly identical DNA sequences (Wells et al., 2009), we expect Ovol2 overexpression to misregulate both Ovol1 and Ovol2 targets. BT animals fed on a Dox-free diet displayed a thinner epidermis than their control littermates (Figure 3A) and died shortly after birth. K15 expression was nearly absent (Figure 3B), and the K1-positive spinous compartment was reduced in size (Figures 3A and 3C). Granular layers and stratum corneum were also smaller but these defects were less remarkable (Figures 3A and 3D; data not shown). Microarray analysis of control and BT embryonic skin revealed a significant downregulation of "stemness" gene sets in the latter (Figure S4B). Furthermore, BT embryonic skin produced dramatically decreased staining for p63 protein (Figure 3E). These alterations suggest reduced epidermal stem/progenitor cells upon Ovol2 overexpression.

HF morphogenesis was affected in a similar manner. The number of HFs in BT embryos was greatly reduced, and the few residual HFs contained shorter trunks, where presumptive HF stem/progenitor cells likely reside (Nowak et al., 2008) (Figures 3A, 3B, and 3F). In contrast, the bulbs of the residual HFs appeared largely normal, and expressed proper lineage differentiation markers including AE13, inner root sheath marker Gata3, and matrix/precortex marker Lef1 (Figures 3F and S4C). Thus, aberrantly elevated Ovol2 expression in embryonic HF epithelial cells diminishes the progenitor cell compartment, while still permitting terminal differentiation.

The molecular similarity between embryonic epidermal progenitor cells and adult HF-SCs (Blanpain and Fuchs, 2009) prompted us to determine whether Ovol2 overexpression affects the latter. To activate transgene expression only in adult skin (specifically in HF ORS/bulge and epidermal basal cells), BT mice were fed a Dox-containing diet during gestation, and Dox was then removed postnatally at different ages (Figure S4D). Upon Ovol2 overexpression, adult BT mice displayed a loss of K15-positive cells in both epidermis and HF bulge (Figure 4A). Furthermore, BT HFs displayed reduced expression of Tcf3 in the bulge and secondary hair germ (HG) (Figure 4B). In contrast, CD34 expression was not affected (Figure S4E). Prolonged transgene expression resulted in hair loss in older BT mice (Figure 4C), and histological analysis confirmed a near-complete absence of HFs; the epidermis was thickened, and the residual

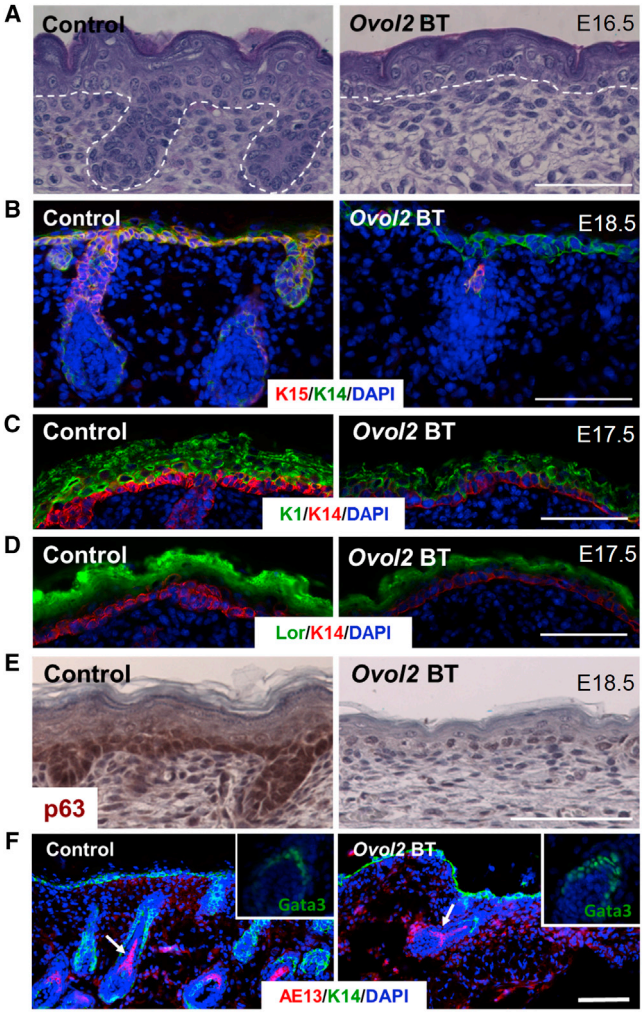

Figure 3. Skin Phenotypes of *Ovol2* BT Embryos

(A) H&E.

(B–D and F) Indirect immunofluorescence of the indicated markers. Slides were double stained for K14, and nuclei were visualized by DAPI.

(E) Immunohistochemistry using a pan-p63 antibody.

Note the presence of AE13-positive cells (arrows in F) in a residual BT HF. Gata3 staining images are shown as insets in (F). Scale bars represent 50 μm.

See also Figure S4.

HFs were epidermalized as shown by aberrant K1 expression (Figure 4D; data not shown).

Adult HFs undergo cyclic bouts of growth (anagen), regression (catagen), and resting (telogen) (Beck and Blanpain, 2012). Proliferation and differentiation of stem/progenitor cells in the bulge/HG drive telogen-to-anagen transition. To examine Ovol2 function in this transition, we activated the *Ovol2* transgene at postnatal day 49 (P49), when HFs are normally in the second telogen. At P63, when HFs in wild-type (WT) mice were still in telogen, HFs in BT littermates had progressed to late anagen (Figure 4E). This was not due to chronic effects of leaky transgene expression (Figure S4F). Collectively, our analyses demonstrate that upon Ovol2 overexpression, adult HFs fail to maintain stem/progenitor cells and undergo precocious differentiation.

Ovol1/Ovol2-Deficient Keratinocytes Exhibit EMT-like Changes Ex Vivo

Our studies above highlight a positive role of *Ovol1/Ovol2* in epidermal differentiation. To seek additional and alternative mechanisms beyond direct repression of *Myc* and *ΔNp63*, we returned to the comparative expression analysis of control and DKO keratinocytes. Remarkably, the expression of a myriad of mesenchymal markers such as *Vim* (vimentin [Vim]) (15×), *Acta2* (smooth muscle actin [SMA]) (10×), *Vcan* (versican) (5×), *Cdh2* (N-cadherin [Ncad]) (4×), and *Fn1* (fibronectin) (3×) was significantly elevated, whereas that of epithelial markers such as *Ocln* (occludin) (18×), *Krt19* (K19) (9×), and *Cdh1* (Ecad) (3×) was significantly reduced in DKO cells (Table S1). RT-PCR confirmed some of these changes (Figure 5A). Moreover, abundant Vim-positive cells, many of which also stained positive for K14, were detected in DKO culture (Figure 5B). The expression of genes encoding EMT-promoting transcription factors, namely *Zeb1* (43×), *Zeb2* (6×), and *Snai2* (Slug) (1.7×), but not *Twist1* and *Snai1*, was dramatically upregulated in DKO cells (Table S1; Figure 5A).

Consistent with EMT-like molecular changes, DKO keratinocytes displayed a tendency to grow as dispersed cells and adopted a fibroblast-like morphology (Figures 2B and 5C). Genotyping revealed near-complete recombination of the floxed *Ovol2* locus (Figure S5A), indicating that these cells were of an epithelial origin. Moreover, DKO cells were significantly more migratory in scratch assays than control (Figure 5D).

Unrestricted epithelial plasticity/EMT may cell autonomously compromise the differentiation potential of epidermal cells. Indeed, Ca^{2+} induced less remarkable differentiation of DKO cells compared to control (Figures 5E and 5F). Even in low-Ca^{2+} medium, where control keratinocytes expressed low but appreciable levels of mRNAs of differentiation genes such as members of the transglutaminase (*Tgm*), late cornified envelope (*Lce*), and small proline-rich protein (*Sprr*) families, DKO cells showed significantly reduced expression of these genes (Table S2). Thus, loss of *Ovol1/Ovol2* renders keratinocytes intrinsically refractory to Ca^{2+}-induced terminal differentiation.

EMT-like Gene Expression and Abnormal Cell Adhesion in *Ovol1/Ovol2*-Deficient Epidermis

To determine whether EMT-like changes occur in vivo, we performed quantitative western blot analysis of freshly isolated embryonic epidermis. The most dramatic elevation was seen for Zeb1, Vim, and SMA, whereas a slight increase was seen for Ncad (Figure 6A). Although only a few scattered Zeb1-positive cells were present at the basal-suprabasal junction of control epidermis, DKO epidermis exhibited an abundant presence of such cells in both basal and suprabasal compartments (Figure 6B). Moreover, whereas occasional Vim-positive cells were detected in the control basal layer, almost all DKO basal cells stained positive for Vim, albeit at a lower intensity compared to the underlying dermis (Figure 6C). The level of *Vim* and *Zeb1* mRNAs was also significantly increased (Figure 6D), suggesting that their upregulation occurs at a transcriptional level. Intriguingly, the mRNA level and staining pattern of Ecad, a well-known Zeb1 target (Peinado et al., 2007), were unaltered in DKO epidermis (Figures 6A and S5B).

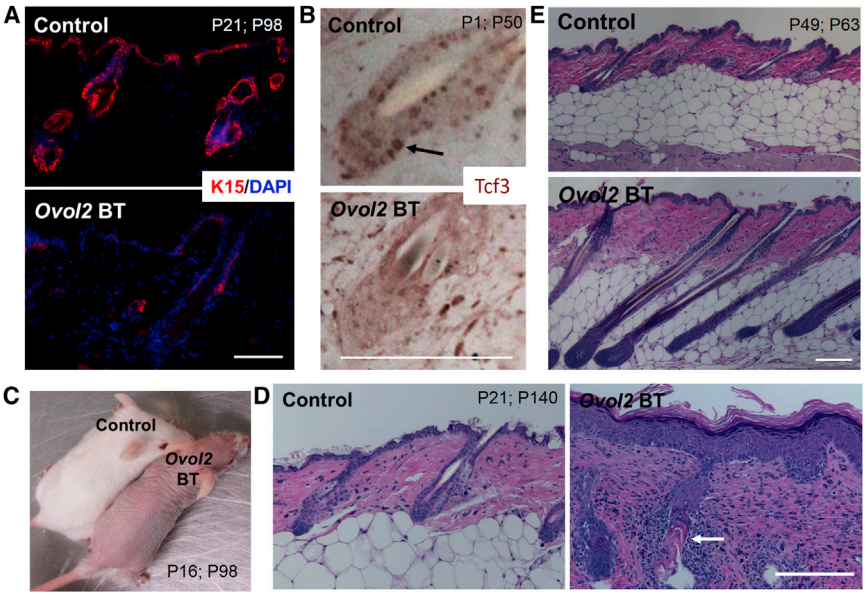

Figure 4. HF Phenotypes of Adult *Ovol2* BT Mice

(A and B) Reduced presence of K15 (A) and Tcf3 (B) proteins in BT skin. Arrow in (B) indicates a Tcf3-positive secondary HG cell.

(C and D) Long-term overexpression of Ovol2 results in loss of hairs (C) and HFs (D). Arrow in (D) indicates the presence of epidermal-like materials in a residual HF.

(E) Precocious progression of BT HFs to anagen. P_; P_ indicates the ages at which BT mice were induced with Dox and taken for analysis. Scale bars represent 50 μm (A, B, and D) and 20 μm (E). See also Figure S4.

To better understand *Ovol1*/*Ovol2* DKO cellular defects in vivo, we returned to EM analysis. Importantly, whereas basal and spinous cells in DKO epidermis were able to form intermittent intercellular bridges/filopodia-like structures and normal-looking desmosomal junctions, they failed to properly "zip" together the intervening membranes to maintain full adhesion to one another (Figure 6E). These defects are strikingly similar to mice deficient in α-catenin, which is required for actin cytoskeleton organization to seal adjacent cell membranes during the formation of stable epidermal cell-cell contacts (Vasioukhin et al., 2000). Consistent with this parallel, the level of α-catenin protein was significantly reduced in DKO epidermis (Figure 6A).

The retention of Ecad in DKO cells in vivo led us to wonder whether artificially enhancing cell-cell contacts in cultured DKO keratinocytes might suppress their EMT-like changes. To address this, we added Ca^{2+}, which induces intercellular adhesion prior to differentiation (Jamora and Fuchs, 2002), to keratinocyte cultures. Consequently, DKO cells no longer exhibited as significant a deviation from the control in their expression of most EMT-related genes, such as *Cdh2*, *Acta2*, and *Snai2* (Table S1). However, the top-affected genes in low Ca^{2+}, such as *Zeb1* and *Vim*, still showed increased expression in DKO cells, albeit to a lesser extent. Importantly, *Ctnna1* (α-catenin) expression was significantly lower in Ca^{2+}-treated DKO cells than control. From these findings, we surmise that (1) the presence of rigid cell-cell organization and differentiation cues in vivo might counterbalance the EMT tendency of *Ovol1*/*Ovol2*-deficient epidermal cells, and (2) misregulation of *Zeb1*, *Vim*, and *Ctnna1* likely represents primary molecular effects of *Ovol1*/*Ovol2* loss, whereas the additional changes that occur only in culture (e.g., reduced *Cdh1* expression) may be secondary.

Zeb1 Mediates Ovol Regulation of *Ctnna1*, EMT, and Terminal Differentiation

We next tested the possibility that Ovol directly regulates EMT-inducing genes in epidermis. Regulatory regions of *Zeb1*, *Vim*, and *Snai2* genes contain Ovol binding motifs, and ChIP experiments revealed Ovol2 binding to the predicted sites in primary keratinocytes (Figure 7A; data not shown). Moreover, the relative binding strength positively correlated with the extent of upregulation in mRNA expression (see above), with *Zeb1* being the most strongly bound and most significantly upregulated. We therefore asked whether depletion of Zeb1 rescues the defects of DKO keratinocytes. Transfection of a *Zeb1*-specific small interfering RNA (siRNA), but not a negative control siRNA, into DKO keratinocytes cultured in low Ca^{2+} resulted in efficient *Zeb1* knockdown (Figure S6A), formation of colonies with epithelial morphology (Figure 7B), and correction of *Fn1*, *Cdh2*, and *Cdh1* mRNA expression to near-control levels (Figure 7C). Importantly, *Ctnna1* mRNA expression was also restored after *Zeb1* knockdown (Figure 7C).

The inverse correlation between *Zeb1* and *Ctnna1* expression led us to examine whether *Ctnna1* is a target of Zeb1 transcriptional repression. Previous ChIP-sequencing (ChIP-seq) studies (University of California at Santa Cruz genome browser) revealed the presence of ZEB1 peaks on the human *CTNNA1* promoter (Figure S6B). Our ChIP experiments revealed Zeb1 binding to the mouse *Ctnna1* promoter in primary keratinocytes (Figure 7D). In reporter assays, cotransfection with a Zeb1 expression construct repressed luciferase activity driven by the *Ctnna1* promoter, but not a mutant promoter where the upstream binding site was mutated (Figure 7E). These data establish *Ctnna1* as a direct target of Zeb1.

Next, we asked whether *Zeb1* depletion affects how *Ovol1*/*Ovol2* deletion impacts cell adhesion and actin dynamics of cultured DKO keratinocytes. Shortly after plating, α-catenin protein was concentrated to the cell borders of control cells that came into close proximity of each other; over several days, the cells eventually sealed together with α-catenin staining remaining strongest at the borders (Figure 7F, left). As expected (Vasioukhin et al., 2000), phalloidin staining revealed actin filaments that localized radially at the periphery of control cells: weak right after plating but enhanced over culturing (Figure 7F, left). In contrast, DKO cells did not show appreciable localization of α-catenin to the cell borders even when they were contacting each other, and abundant stress fibers formed in these cells over time (Figure 7F, middle). When *Zeb1* was depleted, α-catenin localization and actin cytoskeletal staining in DKO keratinocytes resembled control cells (Figure 7F, right). No apparent effect was

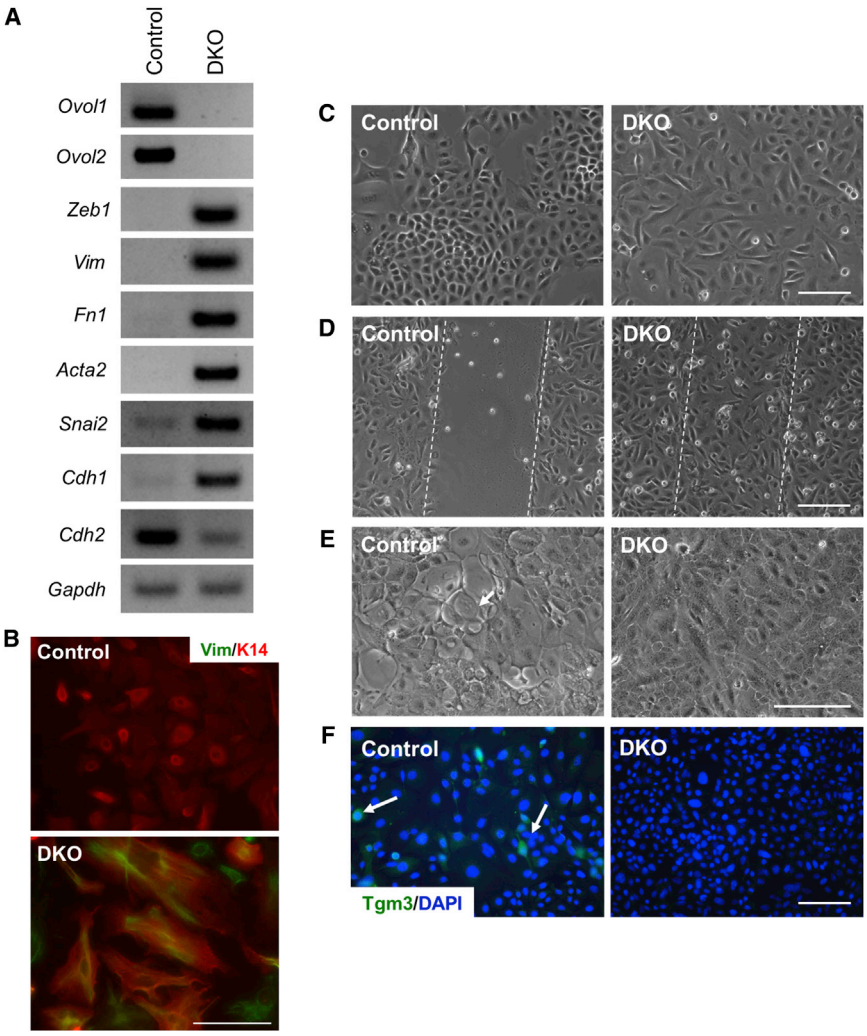

Figure 5. DKO Epidermal Keratinocytes Undergo EMT-like Molecular and Morphological Changes

(A) Semiquantitative RT-PCR. *Gapdh* serves as a loading control.

(B) Increased Vim protein expression in DKO keratinocytes. Shown are merged images with K14 staining.

(C) Morphology of DKO keratinocytes in high-density culture.

(D) Scratch assay. Dashed lines indicate where the scratches were made.

(E) Morphology of Ca^{2+}-treated WT and DKO keratinocytes.

(F) Indirect immunofluorescence of late epidermal differentiation marker transglutaminase 3 (Tgm3) in Ca^{2+}-treated keratinocytes. DAPI stains the nuclei. Arrows in (E) and (F) denote a large, flat differentiated cell and Tgm3-positive cells, respectively.

Scale bars represent 50 μm (B–F). See also Figure S5.

observed when *Zeb1* was depleted in control keratinocytes (data not shown).

Thus, reducing *Zeb1* expression is capable to return *Ovol1*/*Ovol2* DKO keratinocytes to an epithelial state. Is this sufficient to restore their differentiation potential? Indeed, *Zeb1* depletion in DKO keratinocytes led to increased mRNA levels of late epidermal differentiation genes *Tgm1* and *Sprr2j* (Figure 7C), as well as partially rescued the expression of differentiation markers Tgm3 and filaggrin (Figure S6C). In contrast, the expression of self-renewal/proliferation genes *Myc*, *Tcf3*, *Krt15* (K15), and *Itgα6* (α6 integrin) was not affected (Figure S6D). Interestingly, *Zeb1* knockdown resulted in an increased number of colonies formed by DKO keratinocytes while exerting a minimal effect on control cells (Figure 7G). Collectively, our data suggest a model in which Ovol proteins maintain the epithelial identity and differentiation competence of epidermal progenitor cells in part via an Ovol-Zeb1-α-catenin regulatory pathway.

DISCUSSION

Our work underscores Ovol1 and Ovol2 as critically important regulators of epidermal morphogenesis. Overall, they promote terminal differentiation within both epidermal and HF lineages, as well as restrict molecular stem/progenitor cell traits and proliferation potential. Importantly, the study uncovers a previously unrecognized mechanism, where molecular machinery used to regulate epithelial plasticity confers differentiation competence to epidermal progenitor cells.

Although *K14-Cre*-mediated deletion of *Ovol2* results in a near-complete arrest of mammary morphogenesis (Watanabe et al., 2014, this issue of *Developmental Cell*), it severely impacts epidermal differentiation only when *Ovol1* is also deleted (this work). In various assays, *Ovol1*$^{-/-}$ skin either displayed a status that is intermediate between control and DKO or was similar to control, whereas *Ovol2* SSKO skin was indistinguishable from the control (Figures 1, S1, 2, and S2; data not shown). *Ovol1* and *Ovol2* are expressed in distinct but overlapping sites of the developing epidermis. It is possible that under physiological conditions, they each regulate the behavior of distinct subpopulations of epidermal progenitor cells. However, when one is absent, the other is upregulated, reflecting compensatory attempts of the cells to ensure that essential developmental/cellular processes can take place. Proper epidermal differentiation leading to barrier formation is essential for the organism's extrautero survival. Perhaps for this reason, functional compensation/redundancy between *Ovol1* and *Ovol2* is particularly important in developing epidermal progenitor cells.

Interestingly, both reduction and increase in *Ovol* dosage lead to catastrophic consequences, although for different underlying reasons. For example, DKO embryos produce HFs that contain few AE13-positive cells, whereas BT HFs, when formed, seem to generate AE13-positive cells at the expense of HF progenitor cells. These findings imply the need to exquisitely control total Ovol protein levels in skin in order to balance progenitor cell

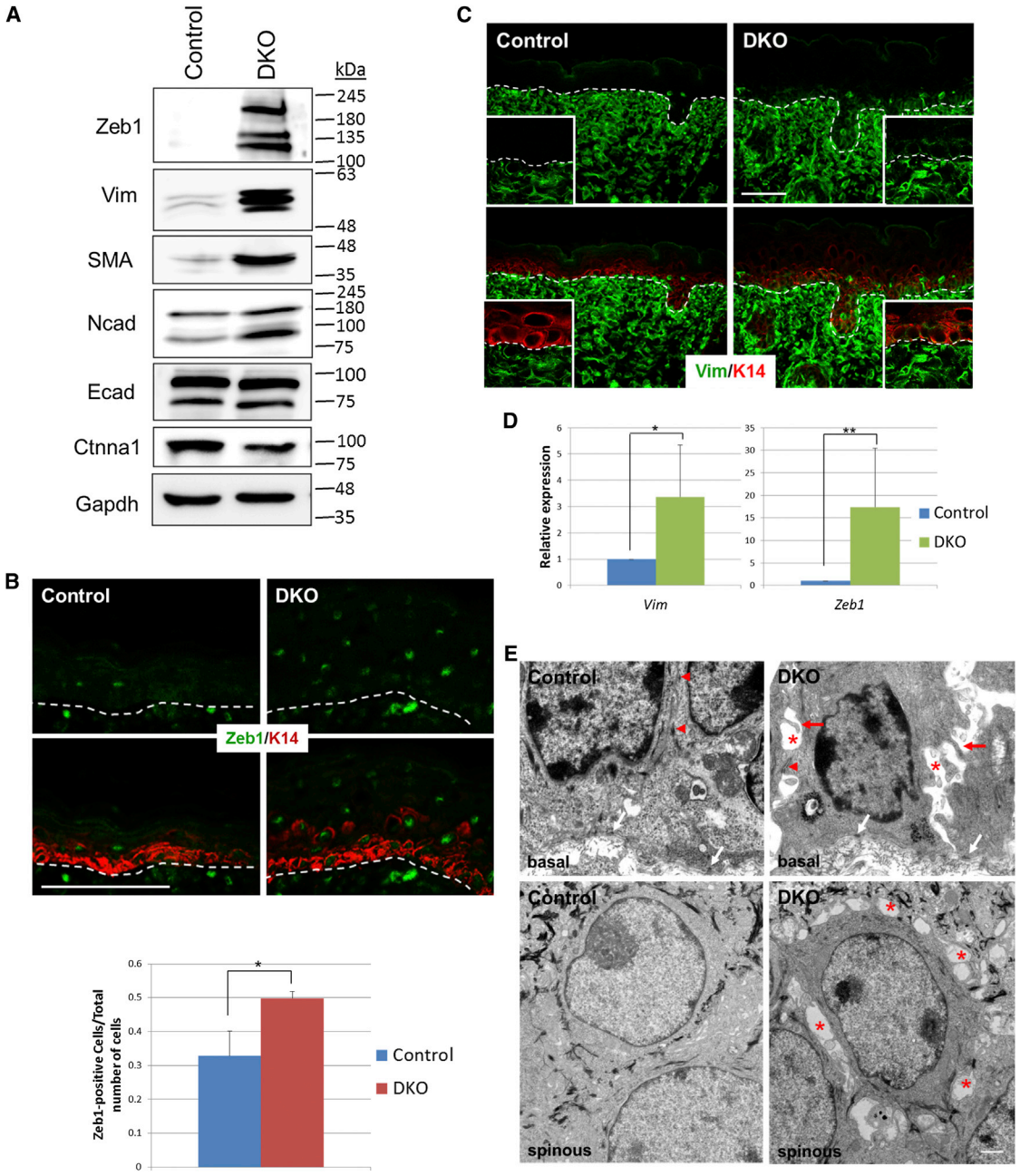

Figure 6. In Vivo EMT-Related Changes in DKO Epidermis

(A) Western blotting analysis of isolated epidermis. Gapdh serves as a loading control. Positions of molecular weight markers are indicated on the right.

(B) Immunofluorescent detection of Zeb1 (top), with quantification of Zeb1-positive cells shown at the bottom (n = 3 per genotype; *p < 0.001). Middle panels are merged images showing Zeb1 and K14 double staining. Note that many cells in the expanded K14-positive zone in DKO skin express Zeb1.

(C) Immunofluorescent detection of Vim. Single-channel (top) and merged (bottom, with K14) images are shown, with high-magnification images included as insets.

(D) RT-qPCR analysis of *Vim* and *Zeb1* mRNAs in epidermis isolated from control and DKO skin. *p = 0.109; **p = 0.096.

(E) EM images showing control and DKO basal (top) and spinous (bottom) cells. Red arrows point to intercellular bridges, red arrowheads point to desmosomes, red stars indicate intercellular gaps, and white arrows point to hemidesmosomes.

Error bars represent SE. Scale bars represent 50 μm (B and C), 5.5 μm (upper panels of E), and 1 μm (lower panels of E).

See also Figure S5.

proliferation with differentiation. Both *Ovol1* and *Ovol2* promoters contain Ovol binding motifs, and Ovol1 autorepresses (Nair et al., 2007; Teng et al., 2007; Wells et al., 2009). These findings suggest that Ovol1 and Ovol2 may mutually repress each other's expression (and autorepress) to maintain adequate total levels of Ovol proteins.

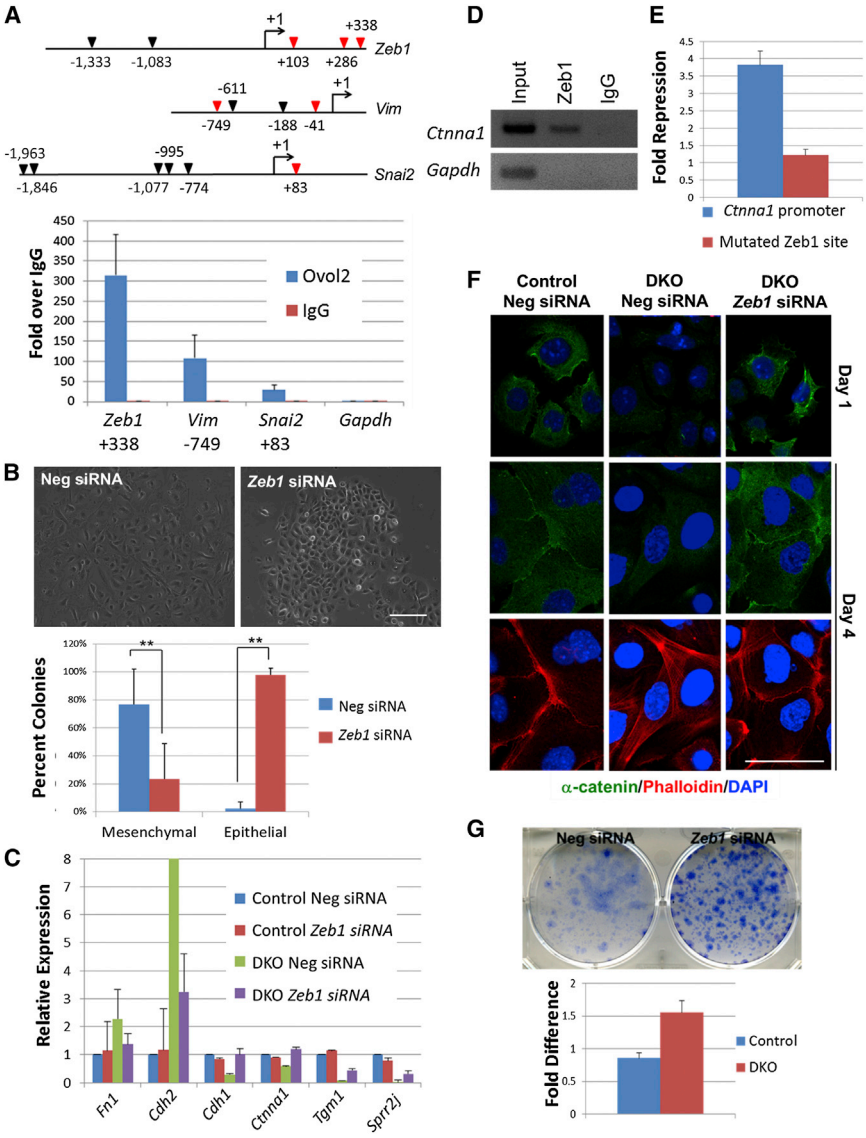

Figure 7. Evidence for an Ovol-Zeb1-α-Catenin Pathway and Zeb1 Importance in *Ovol1*/*Ovol2* DKO Phenotypes

(A) ChIP analysis of Ovol2 on *Zeb1*, *Vim*, and *Snai2* (see legend to Figure 2D for more details).

(B) Morphology (top) and type (bottom) of colonies produced by DKO keratinocytes treated with control (Neg) or *Zeb1* siRNA. **$p < 0.0002$.

(C) RT-qPCR analysis of Neg or *Zeb1* siRNA-treated keratinocytes. *Gapdh* expression was used for normalization.

(D) ChIP revealing Zeb1 binding to *Ctnna1* promoter at predicted sites. The *Gapdh* promoter serves as a negative control.

(E) WT but not mutated *Ctnna1* promoter is repressed by Zeb1 in luciferase reporter assays.

(F) Indirect immunofluorescence of α-catenin and phalloidin on keratinocytes treated with Neg or *Zeb1* siRNA at the indicated time points. Top and middle panels are merged images for α-catenin and DAPI. Bottom panels are merged images for phalloidin and DAPI.

(G) Effect of *Zeb1* knockdown on keratinocyte clonogenicity. Graph depicts fold difference in the number of colonies comparing Neg control siRNA to *Zeb1* siRNA.

Error bars represent SE. Scale bars represent 50 μm (B and F).

See also Figure S6.

Both unipotent embryonic epidermal stem/progenitor cells and multipotent adult HF-SCs display sensitivity to Ovol dosage by altering their gene expression and differentiation programs. Thus, this work adds Ovol1/Ovol2 to the short list of transcription factors including Tcf3, Lhx2, Sox9, and Nfatc1 that regulate the behavior of adult HF-SCs. Interestingly, adult *Ovol2* SSKO mice show a slight delay in anagen entry with incomplete penetrance (data not shown), mirroring the premature progression to anagen observed in *Ovol2* BT mice. Further evidence that Ovol proteins are stem/progenitor cell-limiting factors to facilitate differentiation of adult HF-SCs awaits the generation of appropriate skin-specific *Ovol1*/*Ovol2*-deficient mouse models that do not exhibit perinatal lethality.

Our work mechanistically connects terminal differentiation, EMT, and cell adhesion of epidermal progenitor cells via an Ovol-Zeb1-α-catenin sequential-repression pathway. DKO epidermal cells share the α-catenin deficiency-induced defects in actin cytoskeletal organization and intercellular adhesion (Vasioukhin et al., 2001). Furthermore, like skin-specific *Ctnna1* knockout, DKO mice show hyperproliferative epidermis and defective HF development. That Ovol regulation of α-catenin is mediated by Zeb1 is particularly interesting. Although *Cdh1* has been extensively studied as a Zeb1 target in cancer cells (Peinado et al., 2007), our data showcase α-catenin as the primary effector downstream of Ovol and Zeb1 during epidermal morphogenesis. This function of mammalian Ovol, namely regulating actin cytoskeleton, is somewhat reminiscent of the role of *Drosophila* Ovo (Delon et al., 2003) but with an interesting molecular twist.

It is intriguing to ponder why an inducer of nonepithelial fate is built into the molecular circuit that promotes epithelial adhesion and differentiation. Dynamic changes associated with the adherens junctions provide flexible intercellular adhesions, with transient breakage and reestablishment of adhesive forces likely underlying the proliferative events within the epidermal stem/progenitor cell compartments and the migration of differentiating cells from basal to suprabasal locations (Kobielak and Fuchs, 2004; Watt, 1987). Our study demonstrates that this extremely mild form of epithelial plasticity during epidermal development shares some common molecular features and regulators, such as Ovol and Zeb1, with its more "radical" cousins: EMT and mesenchymal-to-epithelial transition (MET) (Ocaña and Nieto, 2008; Roca et al., 2013). Moreover, Ovol repression of a plasticity inducer (Zeb1) that suppresses epithelial adhesion (α-catenin)

seems a particularly "clever" strategy to ensure a delicate balance between adhesion relaxation and reestablishment. Supporting the broad relevance of this regulation, a spontaneous noncoding point mutation (*Twirler*) in the first intron of *Zeb1* that disrupts a conserved base pair within the +286 Ovol1/Ovol2 binding consensus (Figure 7A) results in inner ear defects (Kurima et al., 2011). Our findings raise the possibility that Zeb1 may normally function in developing epidermis as an adhesion relaxer. The presence of Zeb1 protein at the basal-suprabasal junction is consistent with this notion. Although examination of *Zeb1* null embryonic epidermis did not reveal any apparent anomaly (data not shown), it remains possible that *Zeb2* provides functional compensation.

EMT has recently been shown to promote stem cell properties (Chaffer et al., 2013; Guo et al., 2012; Mani et al., 2008). The fact that *Ovol1/Ovol2*-deficient epidermal cells are EMT prone and "locked" in a proliferative progenitor state seems consistent with this. However, inhibition of EMT by *Zeb1* knockdown in *Ovol1/Ovol2* DKO keratinocytes does not decrease but, instead, increases colony formation. Thus, an epithelial fate is required for maximal clonogenicity, a surrogate measure of stem/progenitor activity of epidermal cells. Ovol1/Ovol2 may also suppress proliferation potential via additional mechanisms independent of Zeb1, α-catenin, or EMT-like events, such as via regulating *Myc* and *p63*. Regardless, our research of Ovol involvement in suppressing both progenitor-like traits and epithelial plasticity paves the way for future studies of their potential role in cancer initiation and metastasis.

EXPERIMENTAL PROCEDURES

Mice

K14-Cre mice, *K5-tTA* mice, floxed (f) and null (–) alleles of *Ovol2* have been described previously by Andl et al. (2004), Diamond et al. (2000), and Unezaki et al. (2007), respectively. *TRE-Ovol2-Flag* transgenic founders were generated by pronuclei injection of CB6F1 mouse eggs at the University of California, Irvine (UCI) Transgenic Mouse Facility. All experiments have been approved by, and conform to the regulatory guidelines of, the UCI International Animal Care and Use Committee.

Immunostaining

For indirect immunofluorescence, mouse back skins were freshly frozen in optimum cutting temperature (OCT) compound (Tissue-Tek) and stained using the appropriate antibodies. The number of $pH3^+$ cells was counted in at least three fields (using ImageJ of skin sections at 10× magnification) per mouse. Immunohistochemical detection of p63 and Tcf3 was performed with paraformaldehyde-fixed paraffin-embedded sections, using Vector ABC (Vector Laboratories; PK-6100) and diaminobenzidine (DAB) (DAKO; K3468) kits per manufacturer's instructions.

Isolation of Epidermis and Culturing of Primary Keratinocytes

Skins of E18.5 embryos were placed with the dermis facing down in Petri dishes with 1 ml of 5 mg/ml dispase (STEMCELL Technologies; 7913) and 1 ml CnT-07 media (CELLnTEC; CnT-07). Skins were incubated in the dispase/media solution at room temperature for 2–4 hr or overnight at 4°C. After incubation, the dermis and epidermis are separated with forceps.

Keratinocytes were isolated from the E18.5 skin of WT and mutant littermates using an established protocol (CELLnTEC). About 2–4 × 10^6 cells were recovered from each mouse and were plated at comparable cell densities among genotypes. The cells were cultured in CnT-02 media (CELLnTEC) with or without addition of 1.2 mM Ca^{2+} for 3–5 days prior to experiments. For clonogenicity assay, cells were plated at 1,000 cells/cm^2 and allowed to grow for 2 weeks, followed by staining with 0.5% methylene blue and 50% ethanol for 30 min. For quantitative analysis, two wells of a 6-well plate were counted and averaged per mouse.

ChIP Assay

ChIP was performed according to the protocol described previously by Dahl and Collas (2008) using primary keratinocytes isolated from newborn control embryos and cultured to reach 70%–80% confluency.

Microarray Analysis

Hybridization of arrays (GeneChip Mouse Exon 1.0 ST Array; Affymetrix) was performed in duplicate using independent biological samples. Affymetrix GeneChip Analysis Suite software (MAS 5.0) was used to generate raw data, and genes with normalized expression levels over detection threshold were called and analyzed for differential expression using the Cyber T program (Long et al., 2001) (http://cybert.ics.uci.edu/).

siRNA Knockdown

Primary mouse keratinocytes were reverse transfected in 6-well plates using Lipofectamine RNAiMAX Transfection Reagent (Life Technologies; 13778-075) according to the manufacturer's recommendations. The following Silencer predesigned siRNAs (Life Technologies) were used at a concentration of 10–25 nM: Silencer Select Negative Control No. 1 siRNA (4390843), and Zeb1 Silencer Select siRNA (4390771). Cells were harvested 24–96 hr after transfection for RNA analysis or up to 2 weeks for morphological analysis.

Additional details for the above procedures, as well as procedures for histology, laser-capture microdissection, RT-PCR, barrier, scratch, and reporter assays, western blotting, GSEA, and statistical analysis, are described in the Supplemental Experimental Procedures.

ACCESSION NUMBERS

The microarray data have been deposited into the GEO database (accession number GSE55075).

SUPPLEMENTAL INFORMATION

Supplemental Information includes Supplemental Experimental Procedures, six figures, and two tables and can be found with this article online at http://dx.doi.org/10.1016/j.devcel.2014.03.005.

ACKNOWLEDGMENTS

We thank the UCI Genomics High-Throughput Facility and Transgenic Mouse Facility for expert service; Yoichiro Iwakura for help in generating *Ovol2* mutant alleles; Julie Segre, Hoang Nguyen, Douglas Darling, Valera Vasioukhin, and Leonard Milstone for antibodies; Sarah Millar for *K14-Cre* mice; and Adam Glick for *K5-tTA* mice. We thank Elaine Fuchs, Bogi Andersen, and Kazuhide Watanabe for critical reading of the manuscript. This work was supported by NIH grants R01-AR47320, R01-GM083089, and K02-AR51482 (to X.D.); NIH grants R01GM67247 and P50GM76516 and NSF grant DMS-0917492 (to Q.N.); and NSF grant DMS-1161621 (to Q.N. and X.D.). B.L. was supported by NIH Systems Biology of Development (T32HD060555) and NIH Translational Research in Cancer Genomic Medicine (T32CA113265) training grants. J.O. was supported by Computational and Systems Biology (T32EB009418) and NIH Systems Biology of Development (T32HD060555) training grants.

Received: January 7, 2013
Revised: January 17, 2014
Accepted: March 12, 2014
Published: April 14, 2014

REFERENCES

Andl, T., Ahn, K., Kairo, A., Chu, E.Y., Wine-Lee, L., Reddy, S.T., Croft, N.J., Cebra-Thomas, J.A., Metzger, D., Chambon, P., et al. (2004). Epithelial Bmpr1a regulates differentiation and proliferation in postnatal hair follicles and is essential for tooth development. Development *131*, 2257–2268.

Beck, B., and Blanpain, C. (2012). Mechanisms regulating epidermal stem cells. EMBO J. *31*, 2067–2075.

Blanpain, C., and Fuchs, E. (2009). Epidermal homeostasis: a balancing act of stem cells in the skin. Nat. Rev. Mol. Cell Biol. *10*, 207–217.

Byrne, C., Tainsky, M., and Fuchs, E. (1994). Programming gene expression in developing epidermis. Development *120*, 2369–2383.

Chaffer, C.L., Marjanovic, N.D., Lee, T., Bell, G., Kleer, C.G., Reinhardt, F., D'Alessio, A.C., Young, R.A., and Weinberg, R.A. (2013). Poised chromatin at the ZEB1 promoter enables breast cancer cell plasticity and enhances tumorigenicity. Cell *154*, 61–74.

Dahl, J.A., and Collas, P. (2008). A rapid micro chromatin immunoprecipitation assay (microChIP). Nat. Protoc. *3*, 1032–1045.

Dai, X., Schonbaum, C., Degenstein, L., Bai, W., Mahowald, A., and Fuchs, E. (1998). The ovo gene required for cuticle formation and oogenesis in flies is involved in hair formation and spermatogenesis in mice. Genes Dev. *12*, 3452–3463.

Delon, I., Chanut-Delalande, H., and Payre, F. (2003). The Ovo/Shavenbaby transcription factor specifies actin remodelling during epidermal differentiation in *Drosophila*. Mech. Dev. *120*, 747–758.

Descargues, P., Sil, A.K., Sano, Y., Korchynskyi, O., Han, G., Owens, P., Wang, X.J., and Karin, M. (2008). IKKalpha is a critical coregulator of a Smad4-independent TGFbeta-Smad2/3 signaling pathway that controls keratinocyte differentiation. Proc. Natl. Acad. Sci. USA *105*, 2487–2492.

Diamond, I., Owolabi, T., Marco, M., Lam, C., and Glick, A. (2000). Conditional gene expression in the epidermis of transgenic mice using the tetracycline-regulated transactivators tTA and rTA linked to the keratin 5 promoter. J. Invest. Dermatol. *115*, 788–794.

Fuchs, E. (2007). Scratching the surface of skin development. Nature *445*, 834–842.

Fuchs, E. (2008). Skin stem cells: rising to the surface. J. Cell Biol. *180*, 273–284.

Fuchs, E., and Nowak, J.A. (2008). Building epithelial tissues from skin stem cells. Cold Spring Harb. Symp. Quant. Biol. *73*, 333–350.

Gomis, R.R., Alarcón, C., He, W., Wang, Q., Seoane, J., Lash, A., and Massagué, J. (2006). A FoxO-Smad synexpression group in human keratinocytes. Proc. Natl. Acad. Sci. USA *103*, 12747–12752.

Guo, D., Xu, B.L., Zhang, X.H., and Dong, M.M. (2012). Cancer stem-like side population cells in the human nasopharyngeal carcinoma cell line cne-2 possess epithelial mesenchymal transition properties in association with metastasis. Oncol. Rep. *28*, 241–247.

Jamora, C., and Fuchs, E. (2002). Intercellular adhesion, signalling and the cytoskeleton. Nat. Cell Biol. *4*, E101–E108.

Jamora, C., Lee, P., Kocieniewski, P., Azhar, M., Hosokawa, R., Chai, Y., and Fuchs, E. (2005). A signaling pathway involving TGF-beta2 and snail in hair follicle morphogenesis. PLoS Biol. *3*, e11.

Kalluri, R., and Weinberg, R.A. (2009). The basics of epithelial-mesenchymal transition. J. Clin. Invest. *119*, 1420–1428.

Kobielak, A., and Fuchs, E. (2004). Alpha-catenin: at the junction of intercellular adhesion and actin dynamics. Nat. Rev. Mol. Cell Biol. *5*, 614–625.

Koster, M.I., Dai, D., and Roop, D.R. (2007). Conflicting roles for p63 in skin development and carcinogenesis. Cell Cycle *6*, 269–273.

Kurima, K., Hertzano, R., Gavrilova, O., Monahan, K., Shpargel, K.B., Nadaraja, G., Kawashima, Y., Lee, K.Y., Ito, T., Higashi, Y., et al. (2011). A non-coding point mutation of Zeb1 causes multiple developmental malformations and obesity in Twirler mice. PLoS Genet. *7*, e1002307.

Li, B., Dai, Q., Li, L., Nair, M., Mackay, D.R., and Dai, X. (2002a). Ovol2, a mammalian homolog of *Drosophila* ovo: gene structure, chromosomal mapping, and aberrant expression in blind-sterile mice. Genomics *80*, 319–325.

Li, B., Mackay, D.R., Dai, Q., Li, T.W., Nair, M., Fallahi, M., Schonbaum, C.P., Fantes, J., Mahowald, A.P., Waterman, M.L., et al. (2002b). The LEF1/beta -catenin complex activates movo1, a mouse homolog of *Drosophila* ovo required for epidermal appendage differentiation. Proc. Natl. Acad. Sci. USA *99*, 6064–6069.

Li, B., Nair, M., Mackay, D.R., Bilanchone, V., Hu, M., Fallahi, M., Song, H., Dai, Q., Cohen, P.E., and Dai, X. (2005). Ovol1 regulates meiotic pachytene progression during spermatogenesis by repressing Id2 expression. Development *132*, 1463–1473.

Lien, W.H., Guo, X., Polak, L., Lawton, L.N., Young, R.A., Zheng, D., and Fuchs, E. (2011). Genome-wide maps of histone modifications unwind in vivo chromatin states of the hair follicle lineage. Cell Stem Cell *9*, 219–232.

Long, A.D., Mangalam, H.J., Chan, B.Y., Tolleri, L., Hatfield, G.W., and Baldi, P. (2001). Improved statistical inference from DNA microarray data using analysis of variance and a Bayesian statistical framework. Analysis of global gene expression in *Escherichia coli* K12. J. Biol. Chem. *276*, 19937–19944.

Mackay, D.R., Hu, M., Li, B., Rhéaume, C., and Dai, X. (2006). The mouse Ovol2 gene is required for cranial neural tube development. Dev. Biol. *291*, 38–52.

Maiden, S.L., and Hardin, J. (2011). The secret life of α-catenin: moonlighting in morphogenesis. J. Cell Biol. *195*, 543–552.

Mani, S.A., Guo, W., Liao, M.J., Eaton, E.N., Ayyanan, A., Zhou, A.Y., Brooks, M., Reinhard, F., Zhang, C.C., Shipitsin, M., et al. (2008). The epithelial-mesenchymal transition generates cells with properties of stem cells. Cell *133*, 704–715.

Mills, A.A., Zheng, B., Wang, X.J., Vogel, H., Roop, D.R., and Bradley, A. (1999). p63 is a p53 homologue required for limb and epidermal morphogenesis. Nature *398*, 708–713.

Mootha, V.K., Lindgren, C.M., Eriksson, K.F., Subramanian, A., Sihag, S., Lehar, J., Puigserver, P., Carlsson, E., Ridderstråle, M., Laurila, E., et al. (2003). PGC-1alpha-responsive genes involved in oxidative phosphorylation are coordinately downregulated in human diabetes. Nat. Genet. *34*, 267–273.

Nair, M., Teng, A., Bilanchone, V., Agrawal, A., Li, B., and Dai, X. (2006). Ovol1 regulates the growth arrest of embryonic epidermal progenitor cells and represses c-myc transcription. J. Cell Biol. *173*, 253–264.

Nair, M., Bilanchone, V., Ortt, K., Sinha, S., and Dai, X. (2007). Ovol1 represses its own transcription by competing with transcription activator c-Myb and by recruiting histone deacetylase activity. Nucleic Acids Res. *35*, 1687–1697.

Nguyen, H., Rendl, M., and Fuchs, E. (2006). Tcf3 governs stem cell features and represses cell fate determination in skin. Cell *127*, 171–183.

Nowak, J.A., Polak, L., Pasolli, H.A., and Fuchs, E. (2008). Hair follicle stem cells are specified and function in early skin morphogenesis. Cell Stem Cell *3*, 33–43.

Ocaña, O.H., and Nieto, M.A. (2008). A new regulatory loop in cancer-cell invasion. EMBO Rep. *9*, 521–522.

Payre, F., Vincent, A., and Carreno, S. (1999). ovo/svb integrates Wingless and DER pathways to control epidermis differentiation. Nature *400*, 271–275.

Peinado, H., Olmeda, D., and Cano, A. (2007). Snail, Zeb and bHLH factors in tumour progression: an alliance against the epithelial phenotype? Nat. Rev. Cancer *7*, 415–428.

Roca, H., Hernandez, J., Weidner, S., McEachin, R.C., Fuller, D., Sud, S., Schumann, T., Wilkinson, J.E., Zaslavsky, A., Li, H., et al. (2013). Transcription factors OVOL1 and OVOL2 induce the mesenchymal to epithelial transition in human cancer. PLoS One *8*, e76773.

Romano, R.A., Smalley, K., Liu, S., and Sinha, S. (2010). Abnormal hair follicle development and altered cell fate of follicular keratinocytes in transgenic mice expressing DeltaNp63alpha. Development *137*, 1431–1439.

Shirley, S.H., Hudson, L.G., He, J., and Kusewitt, D.F. (2010). The skinny on Slug. Mol. Carcinog. *49*, 851–861.

Teng, A., Nair, M., Wells, J., Segre, J.A., and Dai, X. (2007). Strain-dependent perinatal lethality of Ovol1-deficient mice and identification of Ovol2 as a downstream target of Ovol1 in skin epidermis. Biochim. Biophys. Acta *1772*, 89–95.

Thiery, J.P., Acloque, H., Huang, R.Y., and Nieto, M.A. (2009). Epithelial-mesenchymal transitions in development and disease. Cell *139*, 871–890.

Tinkle, C.L., Lechler, T., Pasolli, H.A., and Fuchs, E. (2004). Conditional targeting of E-cadherin in skin: insights into hyperproliferative and degenerative responses. Proc. Natl. Acad. Sci. USA *101*, 552–557.

Unezaki, S., Horai, R., Sudo, K., Iwakura, Y., and Ito, S. (2007). Ovol2/Movo, a homologue of *Drosophila* ovo, is required for angiogenesis, heart formation and placental development in mice. Genes Cells *12*, 773–785.

Vasioukhin, V., Bauer, C., Yin, M., and Fuchs, E. (2000). Directed actin polymerization is the driving force for epithelial cell-cell adhesion. Cell *100*, 209–219.

Vasioukhin, V., Bauer, C., Degenstein, L., Wise, B., and Fuchs, E. (2001). Hyperproliferation and defects in epithelial polarity upon conditional ablation of alpha-catenin in skin. Cell *104*, 605–617.

Watanabe, K., Villarreal-Ponce, A., Sun, P., Salmans, M.L., Fallahi, M., Andersen, B., and Dai, X. (2014). Mammary morphogenesis and regeneration require the inhibition of EMT and terminal end buds by Ovol2 transcriptional repressor. Dev. Cell *29*, this issue, 59–74.

Watt, F.M. (1987). Influence of cell shape and adhesiveness on stratification and terminal differentiation of human keratinocytes in culture. J. Cell Sci. Suppl. *8*, 313–326.

Wells, J., Lee, B., Cai, A.Q., Karapetyan, A., Lee, W.J., Rugg, E., Sinha, S., Nie, Q., and Dai, X. (2009). Ovol2 suppresses cell cycling and terminal differentiation of keratinocytes by directly repressing c-Myc and Notch1. J. Biol. Chem. *284*, 29125–29135.

Woo, W.M., and Oro, A.E. (2011). SnapShot: hair follicle stem cells. Cell *146*, 334–334.e332.

Yang, J., and Weinberg, R.A. (2008). Epithelial-mesenchymal transition: at the crossroads of development and tumor metastasis. Dev. Cell *14*, 818–829.

Yang, A., Schweitzer, R., Sun, D., Kaghad, M., Walker, N., Bronson, R.T., Tabin, C., Sharpe, A., Caput, D., Crum, C., and McKeon, F. (1999). p63 is essential for regenerative proliferation in limb, craniofacial and epithelial development. Nature *398*, 714–718.

Zeller, K.I., Jegga, A.G., Aronow, B.J., O'Donnell, K.A., and Dang, C.V. (2003). An integrated database of genes responsive to the Myc oncogenic transcription factor: identification of direct genomic targets. Genome Biol. *4*, R69.

Zhang, T., Zhu, Q., Xie, Z., Chen, Y., Qiao, Y., Li, L., and Jing, N. (2013). The zinc finger transcription factor Ovol2 acts downstream of the bone morphogenetic protein pathway to regulate the cell fate decision between neuroectoderm and mesendoderm. J. Biol. Chem. *288*, 6166–6177.